

Sliding Mode Control Synthesis For Autonomous Underwater Vehicles

IyakkensemeEkpenyong Okon¹

Department of Electrical/Electronic and Computer Engineering, University of Uyo, Akwalbom, Nigeria

Ozuomba Simeon²

Department of Electrical/Electronic and Computer Engineering, University of Uyo, Akwalbom, Nigeria

simeonoz@yahoo.com

simeonozuomba@uniuyo.edu.ng

Bankole Morakinyo Olumide³

Department of Computer Science Heritage polytechnic IkotUdota, Akwalbom, Nigeria

Abstract— This study presents sliding mode control for autonomous underwater vehicles. In the study, effort is made to eliminate the chattering effect which is harmful to the system actuators. Accordingly, a filtered sliding mode control technique is adopted. In order to ensure the existence of sliding mode, first, a high level commutation control is produced which commutes between two extreme values. Secondly, an integrator which acts as a filter is placed at the output of the control signal. The entire system are then modeled and simulated on Matlab software. The results obtained show that at the output of the sliding mode controller, there is high level of chattering which is the problem tackled in this study. However, at the output of the integrator, smooth signal amplitude is obtained. Essentially, the low pass filter effectively removed the noise signal that causes the chattering. The results published in similar studies which are reviewed in this paper showed that rough amplitude is present in their system response plots and those rough amplitudes are caused by noise. On the other hand, with the approach presented in this paper, by applying the low pass filter to the sliding mode control, the noise is filtered out and the system response plot has smooth amplitude. Hence, the approach employed in this study effectively addressed the challenges present in the previous related studies.

Keywords— Sliding Mode Control, Underwater Vehicles, Chattering Effect, System Actuators, Commutation Control, Control Signal, Low Pass Filter

I. INTRODUCTION

Some decades ago, there was a strong movement towards the development of autonomous underwater vehicles (AUVs) and remotely operated vehicles (ROV) [1,2,3,4]. These two classes of underwater vehicles are intended to provide researchers with simple, long-range, low-cost, rapid response capability to collect pertinent environmental data. There are numerous applications for AUV and ROV, including underwater structure inspection, oceanographic surveys, operations in hazardous

environments, and military applications. In order to fulfill these objectives, the vehicles must be provided with a set of controllers assuring the desired type of autonomous operation and offering some aid to the operator, for vehicles which can be tele-operated [5,6,7].

In any case, the automatic control of underwater vehicles presents a difficult design problem due to the nature of the dynamics of the system to be controlled. Controllers based on the simple models of vehicle mass and drag usually yield disappointing performances [8]. The general underwater vehicle control system design problems include a variety of nonlinearities and modelling uncertainties. These include hydrodynamic nonlinearities, inertial nonlinearities, and problems related to coupling between the degrees of freedom (DoF). Simple control techniques such as proportional, integral and derivative (PID) control have been more commonly used because of the relative ease of implementation. A PID tracking controller has been implemented successfully on an unmanned underwater vehicle (UUV) [9,10,11,12,13]. The PID controller is an extension of the control technique of computed torque control which is used in robotics. Simple linear quadratic Gaussian controllers have also been developed [14]. Despite the existence of these simple controllers, other more sophisticated control techniques have also been recently utilized for UUVs. Fuzzy logic controllers (FLCs) have been proposed and implemented with success on UUVs in several cases [15]. The different control techniques discussed have more commonly been used in combination with one another. For instance, a neuro-fuzzy controller has been developed by [16] for modelling attitude control for an UUV. This involved using a combination of neural networks and fuzzy logic. Despite all these however, the desired efficacy has not been realized. Particularly, the chattering effect which has extreme adverse effect on the system actuators has not been effectively addressed by any of these methods. Consequently, this paper presents an filtered sliding mode control (FSMC) technique which uses the a low pass filter to eliminate the chattering effect which is caused by noise that is present in the control variable. The relevant mathematical models and numerical computations are used to demonstrate the effectiveness of the (FSMC) technique in eliminating the chattering effect UUV.

II. METHODOLOGY

A. SLIDING MODE STRUCTURES

The sliding mode structure where commutations occur in the control unit with the addition of the equivalent control was adopted in this research. In order to ensure the existence of the sliding mode, a high level commutation control was produced. Also, the control structure depicted in Figure 1 is adopted where an integrator is placed in front of the system to be controlled, specifically to ensure that chattering is eliminated. A sliding mode control, ω is then derived for the extended system (the original system plus the integrator). The control signal, ω is not “chattering-free”, but the true control signal u going into the system is smooth since the high frequency chattering in ω is filtered out by the integrator, which acts as a low pass filter. With such a design, the chattering reduction was achieved by using the low pass filter and at the same time the control accuracy is maintained.

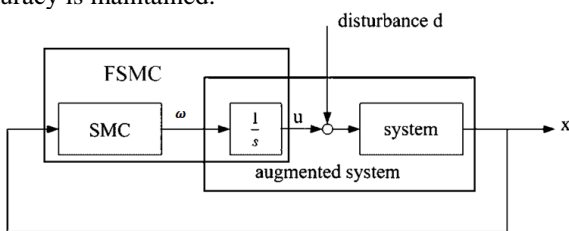


Figure 1: Filtered Sliding Mode Control (FSMC)

Source: Designed by the Researcher

As shown in Figure 1 the system consists of three primary blocks which were nested to form two secondary blocks. The primary blocks are, the sliding mode control (SMC) block, the integrator (low pass filter) block and the system block. The sliding variable in the sliding mode control design is chosen such that the control input showed up in the time derivative of the sliding variable. In this way, the control input is able to influence how the sliding variable evolved. In other words, the time derivative of the new sliding variable for the extended system contains the sliding mode control, ω . This shows that the new sliding variable for the extended system contains the integration of ω which is the true control signal, u . Since the disturbance, d is expected in the system in the same place as the control signal, u , the output of the system is also expected to contain the elements the disturbance, d and this made evaluation of the sliding variable difficult. This formed a problem that is unique to the low-pass-filtering design. A variable structure estimator is then deployed to estimate the sliding variable; this is based on the assumption that the system state is uniformly bounded before proving the system stability.

B. THE SLIDING VARIABLE DESIGN

The control structure of the Filtered Sliding Mode Control is depicted in Figure 1. An integrator was introduced before the system and $\omega = \dot{u}$ was treated as the control variable for the extended system. A switching sliding mode control law was chosen for ω to suppress the effects of disturbance, d . In other words, the new control design removes chattering by filtering the control signal, hence, the control structure in (Figure 1) was termed the

filtered sliding mode control (FSMC). The sliding mode control design for a nonlinear system with uncertainty was used and it is given as:

$$\dot{x} = Ax + B(u + d) \quad (1)$$

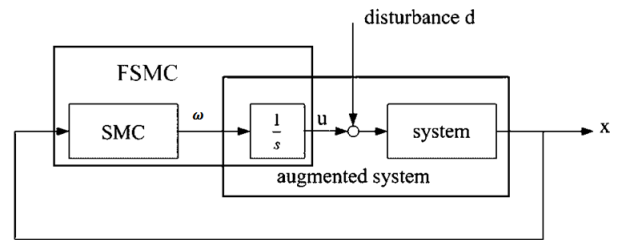


Figure 1: Filtered Sliding Mode Control (FSMC)

Source: Designed by the Researcher

where: $x \in R^n$ is the system state, $u \in R^1$ is the scalar control input, and d is the external disturbance. The system state, x is accessible for measurement, and (A, B) is controllable. For simplicity, it the system uncertainty d is assumed to be a bounded external disturbance and the sliding variable is given as follows;

$$\left. \begin{aligned} \sigma &= \dot{z} + \lambda z \\ z &= Cx \end{aligned} \right\} \quad (2)$$

where: λ is a positive constant, σ is the sliding variable and the row vector $C \in R^{1 \times n}$ was chosen such that (A, B, C) is of relative degree one and the $(n - 1)$ zeros of the system (A, B, C) are in the stable location. When σ tends to zero, the system state x converges to zero. Combining Equation (1) and Equation (2) gives:

$$\sigma = CAx + CB(u + d) + \lambda Cx \quad (3)$$

The time derivative of the sliding variable (Equation (1)) is given as follows;

$$\dot{\sigma} = A\dot{x} + B(\dot{u} + \dot{d}) \quad (4)$$

Substituting Equation (1) into Equation (4) gives;

$$\dot{\sigma} = A^2x + BA(u + d) + B(\dot{u} + \dot{d}) \quad (5)$$

The derivative of the sliding variable σ is taken to be of the form;

$$\dot{\sigma} = \dot{z} + \lambda \dot{z} \quad (6)$$

In order to derive the time derivative of the sliding variable), Equation (1) and Equation (5) are substituted into Equation (6) to give;

$$\dot{\sigma} = C[A^2x + BA(u + d) + B(\dot{u} + \dot{d})] + \lambda C[Ax + B(u + d)] \quad (7)$$

Multiplying out and collecting the like terms in Equation (7) and substituting $\dot{u} = \omega$ into Equation (7) gives;

$$\dot{\sigma} = (CA^2 + \lambda CA)x + (CBA + \lambda CCB)u + CB\omega + (CBA + \lambda CCB)d + CB\dot{d} \quad (8)$$

Obviously, the control variable $\omega = \dot{u}$ appears in the time derivative of the sliding variable, $\dot{\sigma}$ which means that the evolution of $\dot{\sigma}$ can be controlled by properly choosing the control variable, ω . However, there was a challenge according to Equation (3), the expression of $\dot{\sigma}$ contains the unknown disturbance term, d . Therefore, it becomes difficult to evaluate the sliding variable, $\dot{\sigma}$. In order to solve this problem, the disturbance estimator proposed in [17] is used to estimate the disturbance d . With an estimate of d , it becomes possible to obtain an estimate of the sliding variable, $\dot{\sigma}$ through Equation (3). As a result, an estimator for the unknown disturbance d is derived based on the

scalar variable, z defined in Equation (2) where the scalar variable, z satisfies the following differential equation;

$$\dot{z} = CAx + CB(u + d) \quad (9)$$

An estimate of z is taken to be \hat{z} , and the estimator error denoted as e is given as follows;

$$\left. \begin{aligned} e &= z - \hat{z} \\ z &= Cx \end{aligned} \right\} \quad (10)$$

The governing equation of \hat{z} is given as;

$$\left. \begin{aligned} \dot{\hat{z}} &= CAx + \beta e + CB(u + v) \\ v &= \rho \left(\frac{e}{|e| + \varepsilon} \right) \end{aligned} \right\} \quad (11)$$

where: β is a positive constant, ρ an estimator gain which must be larger than the disturbance upper bound, D_0 , and ε is a positive constant close to zero. The estimate of the disturbance, \hat{d} is given as;

$$\hat{d} = \frac{\beta}{CB} e + v = \frac{\beta e}{CB} + \rho \frac{e}{|e| + \varepsilon} \quad (12)$$

Then, σ is approximated as follows;

$$\hat{\sigma} = CAx + CB(u + \hat{d}) + \lambda Cx \quad (13)$$

The effectiveness of the disturbance estimator is assessed in terms of the values of the disturbance estimation error, which is given as $d - \hat{d}$. Accordingly, the disturbance estimation error will become arbitrarily small if the gain ρ is sufficiently large. Now, from Equation (10), \dot{e} can be given as;

$$\dot{e} = \dot{z} - \dot{\hat{z}} \quad (14)$$

Substituting Equation (9) and Equation (12) into Equation (14) gives;

$$\dot{e} = [CAx + CB(u + d)] - [CAx + \beta e + CB(u + v)] = -\beta e - CB(v - d) \quad (15)$$

Substituting the value of v from Equation (11) into

Equation (15) gives;

$$\dot{e} = -\beta e - CB \left(\rho \frac{e}{|e| + \varepsilon} - d \right) = CBd - (\beta e + CB \rho \frac{e}{|e| + \varepsilon}) \quad (16)$$

It is then checked to ensure that both e and \dot{e} become arbitrarily small if ρ is sufficiently large. In that case, from Equation (16);

$$\dot{e} = CB(d - \hat{d}) \quad (17)$$

This implies that \dot{e} tends to zero as $d - \hat{d}$ tends to zero, hence the effectiveness of the disturbance estimation is ascertained.

C. CONTROL VARIABLE DESIGN

In the filtered sliding mode control, the control variable ω is used to drive the sliding variable, σ as close to zero as possible in the face of system uncertainties. For this purpose, the choice of $\dot{u} = \omega$ is made. Hence;

$$\dot{u} = -(CA^2 + \lambda CA)x - (CBA + \lambda CB)u - \gamma\sigma - \delta \text{sgn}(\sigma) \quad (18)$$

where: $\gamma > 0$, $\text{sgn}(\cdot)$ is the signum function, and δ is an upper bound of uncertainty $|\Delta p|$, with

$$\Delta p = (CBA + \lambda CB)d + \dot{d} \quad (19)$$

Based on the preceding mathematical expressions, it is impossible to evaluate the sliding variable, σ due to the uncertainty, d involved. Hence, to implement the proposed control, the estimate, $\hat{\sigma}$ is used in place of σ . On this note, \hat{u} is given as;

$$\hat{u} = \omega = -(CA^2 + \lambda CA)x - (CBA + \lambda CB)u - \gamma\hat{\sigma} - \delta \text{sgn}(\hat{\sigma}) \quad (20)$$

where: $\hat{\sigma}$ is defined in Equation (13). Then, from Equation (20), the actual input to the system is given by;

$$\left. \begin{aligned} u &= H(s)\omega \\ H(s) &= \frac{1}{s} \end{aligned} \right\} \quad (21)$$

Even though the switching control, ω in Equation (20) contains high-frequency chattering, the high-frequency

chattering is filtered by the low-pass filter, $H(s)$. The control input, u to the system is then obtained by direct integration which makes it to become chattering free.

D. VALIDATION OF THE SLIDING VARIABLE

In order to prove the effectiveness of the disturbance estimator given by Equation (12), theorem 1 is propounded.

Theorem 1: The disturbance estimation error, $d - \hat{d}$, where \hat{d} is given by Equation (12), will become arbitrarily small if the estimator gain ρ in Equation (11) is sufficiently large.

Proof: Subtracting Equation (11) from Equation (9) yields:

$$\dot{e} = -\beta e - CB \left(\rho \frac{e}{|e| + \varepsilon} - d \right).$$

It was stated in Equation (17) that $\dot{e} = CB(d - \hat{d})$. This implies that \dot{e} is driven to zero as $d - \hat{d}$ tends to zero; this proves the effectiveness of disturbance estimation.

E. VALIDATION OF THE CONTROL VARIABLE

In order to prove the stability of the control variable, theorem 2 is propounded.

Theorem 2: The proposed filtered sliding mode control in Equation (20) practically stabilizes the system shown in Equation (1) with bounded control, u in the sense that the system state is asymptotically driven into a residual set around the origin, with the size of residual set becoming arbitrarily small when the estimator gain, ρ in the disturbance estimator shown in Equation (11) becomes sufficiently large.

Proof: Denote $\tilde{\sigma} = \sigma - \hat{\sigma}$, where σ and $\hat{\sigma}$ are as given by Equation (3) and Equation (13) respectively. By inspection, it is obvious that $\tilde{\sigma} = CB(d - \hat{d})$. In order to study the evolution of σ , a Lyapunov function, $V = \frac{1}{2}\sigma^2$ is selected and its time derivative under the proposed condition, ω in Equation (20) is checked.

$$\dot{V} = \sigma\dot{\sigma} \quad (22)$$

$$\dot{V} = \sigma[(CA^2 + \lambda CA)x + (CBA + \lambda CB)u + CB\omega + (CBA + \lambda CB)d + CB\dot{d}] \quad (23)$$

$$\dot{V} = \sigma[-\gamma\hat{\sigma} - \delta \text{sgn}(\hat{\sigma}) + \Delta p] \quad (24)$$

$$\dot{V} = \sigma[-\gamma(\sigma - \tilde{\sigma}) - \delta \text{sgn}(\hat{\sigma}) + \Delta p] \quad (25)$$

$$\dot{V} = -\gamma\sigma^2 + \gamma\sigma\tilde{\sigma} + \sigma[-\delta \text{sgn}(\hat{\sigma}) + \Delta p] \quad (26)$$

where: Δp is as given in Equation (19), and $\hat{\sigma} = \sigma - \tilde{\sigma}$ is used to obtain Equation (25) from Equation (24). Suppose $|\sigma| > |\tilde{\sigma}|$; in this case, $\text{sgn}(\hat{\sigma}) = \text{sgn}(\sigma - \tilde{\sigma}) = \text{sgn}(\sigma)$. Equation (26) then becomes:

$$\dot{V} \leq -\gamma\sigma^2 + \gamma\sigma\tilde{\sigma} - |\sigma|(\delta - |\Delta p|) \quad (27)$$

$$\dot{V} \leq -\gamma\sigma^2 + \gamma\sigma\tilde{\sigma} \quad (28)$$

$$\dot{V} \leq -\gamma|\sigma|^2 + \gamma|\sigma|\mu \quad (29)$$

Where Equation (28) results from the design choice $\delta > |\Delta p|$, and in Equation (29), μ as an arbitrarily small number is there due to the fact that $\tilde{\sigma} = CB(d - \hat{d})$ becomes arbitrarily small asymptotically. From Equation (29), it is obvious that $\lim_{t \rightarrow \infty} |\sigma| \leq \mu$, that is σ becomes arbitrarily small asymptotically.

E. PROOF OF CONCEPT

The system given in Equation (1), where $\dot{x} = Ax + B(u + d)$ is considered for the numerical computation. The parameters are taken from (Vervoort, 2009) as follows;

$A = \begin{bmatrix} 2 & 0 \\ 1 & 0 \end{bmatrix}$, $B = \begin{bmatrix} 1 \\ 0 \end{bmatrix}$, $d = 0.9\sin(628t)$ and $d_{max} = 0.9$, the state feedback gain $K = [83.88 \ 112.91 \ 52.71 \ 15.10]$, small boundary layer $\varepsilon_1 = 0.5$, $\rho_1 = 1.2$, $\lambda = 2$, $\beta = 100$, $\delta = 16.08$, $\sigma = [1 \ 1]$, $C = [1 \ 1]$ and $\mu = 0.5$. These parameters are computed using Matrix Laboratory (MATLAB).

III. RESULTS AND DISCUSSION

The phase plane trajectory plot is shown in Figure 2. From the phase plane trajectory plot, it is seen that the

trajectory starts from the initial point (1, 1), move towards the switching surface $x_1 + x_2 = 0$, then slide along the surface to reach the equilibrium point $x = 0$. The state of system response is presented in Figure 3 and Figure 4. According to Figure 3 and Figure 4, both signal x_1 and x_2 reach 0 after about 7 seconds. Also, the trajectory of x_1 plot in Figure 3 reaches the switching surface when the time is approximately 1.4 seconds.

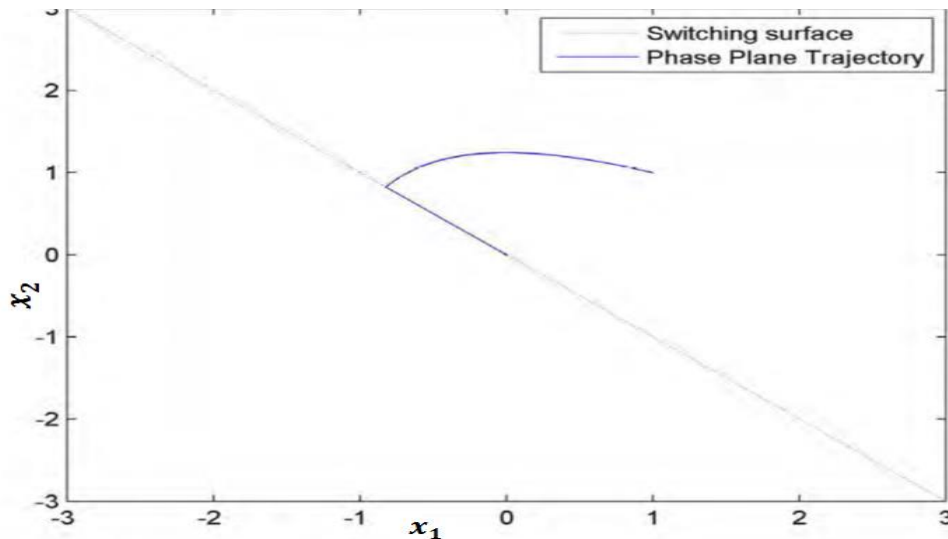


Figure 2: Phase plane trajectory of the system response for $x_1(0) = x_2(0) = 1$ as initial condition

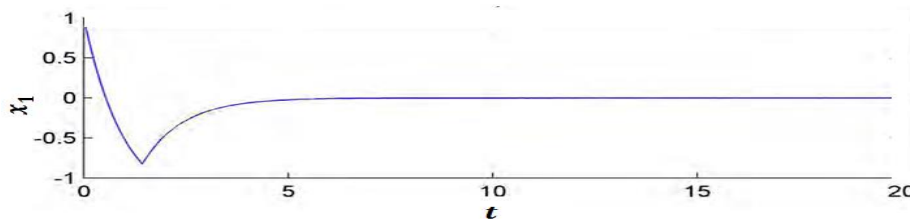


Figure 3: State x_1 of the system response for $x_1(0) = 1$

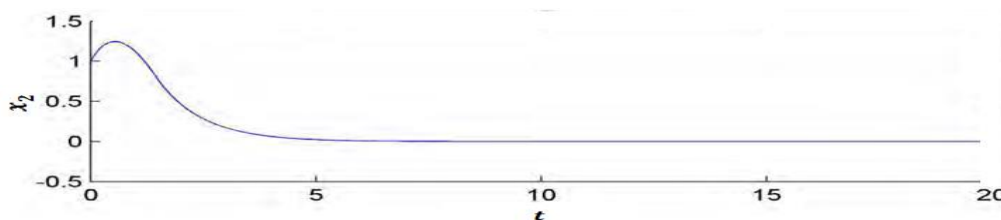


Figure 4: State x_2 of the system response for $x_2(0) = 1$

The control signal response is shown in Figure 5. In Figure 5, the control signal at one instant is a positive number and at another instant is a negative number. This is due to the use of sign function in the control law. Switching between positive and negative small number of σ will cause the control signal $u(t)$ to fluctuate along the envelope of the signal, with the fluctuation amplitude of 1.4 units as confirmed from the plot.

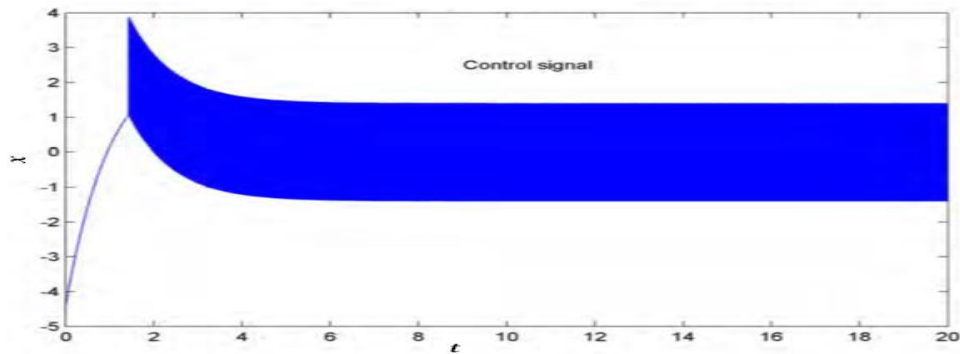


Figure 5: Control signal of the system response for $x_1(0) = x_2(0) = 1$ as initial condition

Simulation result for the phase plane trajectory with different initial conditions given as $x_1(0), x_2(0) \leq 2$ is as shown in Figure 6.

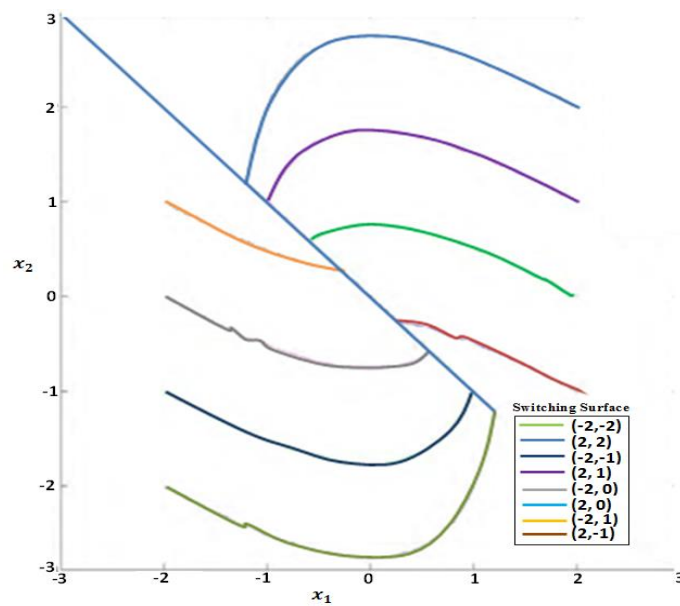


Figure 6: Phase plane trajectory of the system response for the initial conditions given as $x_1(0), x_2(0) \leq 2$

In Figure 6, the trajectories start from the initial conditions and move towards the switching surface. The state of the system response for the same initial conditions given as $x_1(0), x_2(0) \leq 2$ is shown in Figure 7. The y-axis

represents the states x_1 and x_2 while the x-axis represents time.

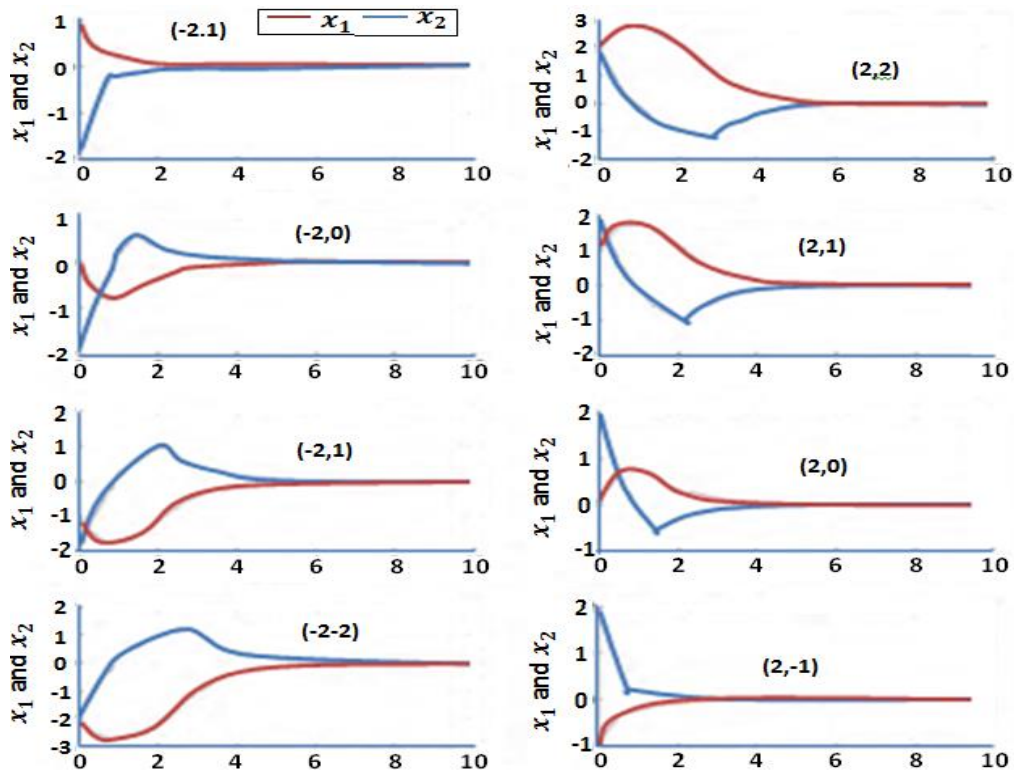


Figure 7: State x_1 and x_2 of the system response for different $x_1(0)$ and $x_2(0)$ as initial conditions

It is observed in Figure 7 that the state of the system response is driven towards the equilibrium point in the switching surface for any initial condition. The control

signal response for the given initial condition $x_1(0), x_2(0) \leq 2$ is presented in the sub plots in Figure 8.

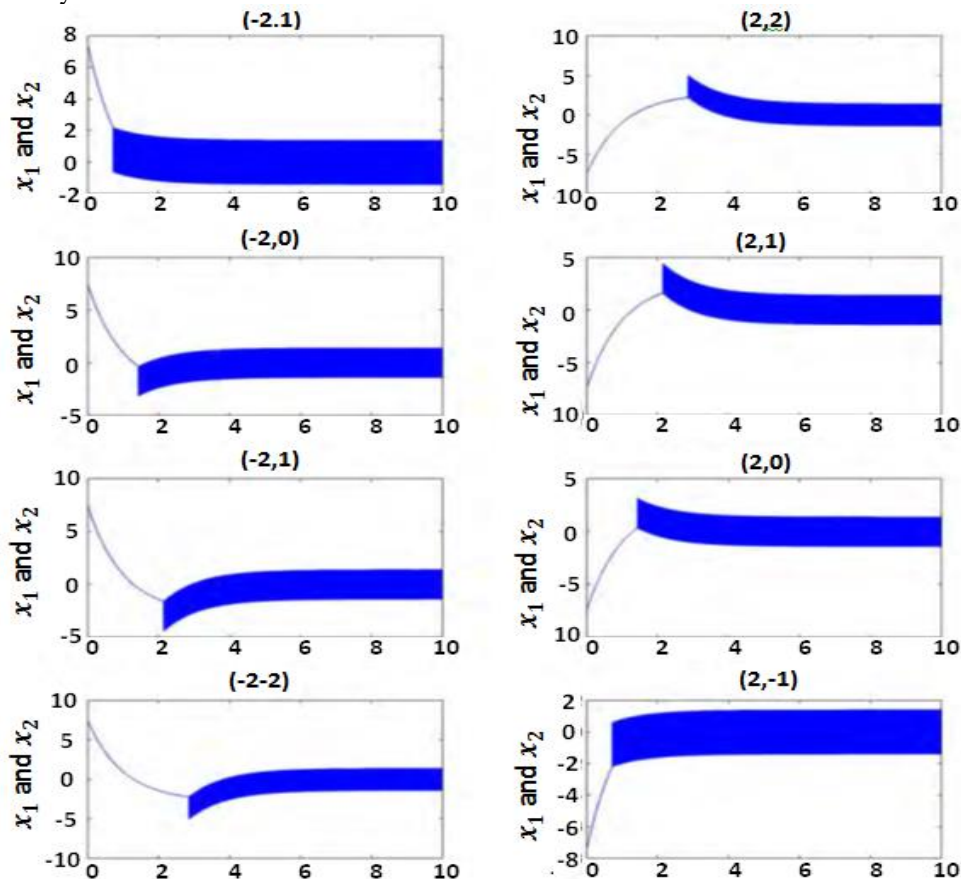


Figure 8: The control signal response for the given initial condition $x_1(0), x_2(0) \leq 2$

Just as it was observed in Figure 4, Figure 7 also shows that the control signal at one instant is a positive number, and at another instant is a negative number. This is due the use of sign function in the control law. However, if the system is assumed to be an ideal one, the amplitude of the switching signal tends to zero, as shown in Figure 9.

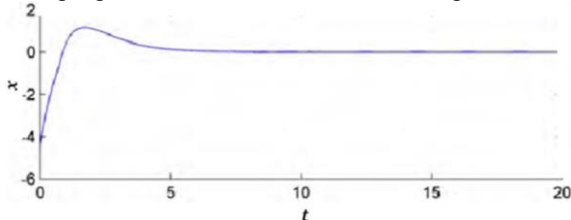


Figure 9: Sliding mode control without noise

The parameters used for the simulation were taken from (Vervoort, 2009). In Figure 9, the trajectory of the control signal swings and settles around zero. The signal remains on the surface for all $t \geq 5$ seconds. This stability of the signal around the equilibrium point is possible due to the fact that the system is assumed to be ideal with no noise element. With this conception, many control approaches will work. For instance, a similar result as shown in (Vervoort, 2009), where boundary layer technique was used for the design. Unfortunately, noise is inevitable in the real world design; this implies that the control signal will always tend to move away from the equilibrium region. This scenario requires a robust control to keep the control signal in the equilibrium region. The parameter chosen for the noise is a sinusoidal function and it is given as $d = \cos(2t)$. In Figure 4 and Figure 7, it is obvious that the trajectory of the signal is not as close to the equilibrium point as when there was no noise in the system. In the real sense, when noise is introduced to the system, the trajectory drifts away from the equilibrium region. The control law was synthesized to drive this error to zero to ensure that the trajectory returns as soon as possible to equilibrium. This routine causes the trajectory to assume a zigzag path, and oscillates in high frequency. As seen in Figure 5 and Figure 8, the trajectory assumes uniform amplitude which minimizes the chattering phenomenon. The results published in similar studies, [18] and [19] showed that rough amplitude is present in their system response plots and those rough amplitudes caused by noise do cause severe harmful effect to the system's actuators. On the other hand, with the approach presented in this paper, by applying a filter to the sliding mode control, the noise is filtered out and the system response plot has smooth amplitude. Hence, the approach employed in this study effectively addressed the challenges present in previous related studies.

IV. CONCLUSION

In this paper, a filtered sliding mode control technique is used to eliminate the chattering effect which is harmful to the system actuators of autonomous underwater vehicles. The filtered sliding mode control technique adopted in this study has proven its robustness based on the results obtained. The new design required estimation of the sliding variable since the value of disturbance may not be exactly known on real time, and this has been achieved by the use

of a disturbance estimator. In order to optimize chattering reduction, sufficiently large disturbance estimator gain was necessary. Based on the selected parameters for the simulations, unnecessary overshoots were removed. It is obvious that with the given control law, the system trajectories are always forced towards the equilibrium point on the sliding surface given any initial values.

REFERENCES

1. Slotine, J. E. (1991). *Application of Sliding Mode Control to Autonomous Underwater Vehicles*. Allen Press, California, pp. 52 – 71.
2. Blidberg, D. R. (2001, May). The development of autonomous underwater vehicles (AUV); a brief summary. In *IeeeIcra* (Vol. 4, p. 1).
3. Smallwood, D., Bachmayer, R., & Whitcomb, L. (1999, September). A new remotely operated underwater vehicle for dynamics and control research. In *Proceedings of the 11th International Symposium on Unmanned Untethered Submersible Technology* (pp. 370-377).
4. Yusoff, M. A. M., & Arshad, M. R. (2013). Development of a Remotely Operated Vehicle (ROV) for underwater inspection. *Jurutera*, 2, 10-13.
5. Fong, T., & Thorpe, C. (2001). Vehicle teleoperation interfaces. *Autonomous robots*, 11(1), 9-18.
6. Reshmi, K. R. G., & Priya, P. S. Design and Control of Autonomous Underwater Vehicle for Depth Control Using LQR Controller. *International Journal of Science and Research (IJSR)* Volume 5 Issue 7, July 2016 Available at : <https://pdfs.semanticscholar.org/7b41/a7841b26ad89a6d48d63b9bd359fd74c560e.pdf> Accessed on 10th July 2018
7. Levant, A. (1999). Underwater Vehicle Behavior and their Incorporation into Control System Design. *Beijing Qing*, 16(28): 74 - 91.
8. Goheen, K. R. and Jefferys E.R. (2009). Application of Alternative Modelling Techniques to RoV Dynamics. *Talanta*, 14(10): 1302-1309.
9. Kawamura, L. Z. (1994). *From First Order to Higher Order Sliding Mode*. Prentice-Hall, London, pp. 212 - 280.
10. Gonzalez, L. A. (2004). Design, modelling and control of an autonomous underwater vehicle. *BE Thesis, The University of Western Australia, Australia*.
11. Yildiz, Ö., Gökcalp, R. B., & Yilmaz, A. E. (2009, November). A review on motion control of the underwater vehicles. In *2009 International Conference on Electrical and Electronics Engineering-ELECO 2009* (pp. II-337). IEEE.
12. Lea, R. K., Allen, R., & Merry, S. L. (1999). A comparative study of control techniques for an underwater flight vehicle. *International Journal of Systems Science*, 30(9), 947-964.
13. Watson, S. A., & Green, P. N. (2014). Depth control for micro-autonomous underwater vehicles (μ AUVs): Simulation and experimentation.

-
- International Journal of Advanced Robotic Systems*, 11(3), 31.
14. Plotnik, A. M. and Rock, S. M. (2007). *Multi-sensor Approach to Autonomous Underwater Vehicle Tracking*. Heinemann Educational Books, London, pp. 76 - 152.
 15. Yokto, L. Y. (2005). Sliding Mode Control for Non Linear Systems. *Talanta*, 3(6): 22 – 54.
 16. Kheuz, L. C. (2003). Problem Identification for Underwater Remotely Operated Vehicle. *Talanta*, 2(5): 12 – 24.
 17. Bartolini, G. and Pydynowski, P. (2006). An improved Chattering Free Scheme for Uncertain Dynamical Systems. *Mainland Press*, 12(14): 54 – 72.
 18. Vervoort, J. H (2009). *Modelling and control of Unmanned Underwater Vehicle*. Springer Verlag, New York, pp. 45 - 83.
 19. Moldoveanu, S. R. (2014). Sliding Mode Controller Design for Robot Manipulators. *Transilvania*, 26 – 39.